Citation: Martínez-Lopez, M.R., 2023. Study of the rupture processes of the 1989 (Mw 6.9) and 2021 (Mw 7.0) Guerrero earthquakes using teleseismic records: Seismotectonic implications. Geologica Acta, 21.9, 1-14.
DOI: 10.1344/GeologicaActa2023.21.9

geologica acta

Study of the rupture processes of the 1989 (Mw 6.9) and 2021 (Mw 7.0) Guerrero earthquakes using teleseismic records: Seismotectonic implications

María del Rosario Martínez-López

Universidad Nacional Autónoma de México, Instituto de Geofísica
Circuito de la Investigación Cientítifca s/n, Ciudad Universitaria, Delegación Coyoacán, Ciudad de México, México 04510

ABSTRACT

Slip models of the April 25, 1989 (Mw 6.9) earthquake and the Acapulco earthquake of September 8, 2021 (Mw 7.0) were determined to analyze its rupture zone and understand the relationship of interplate earthquakes in the Acapulco–San Marcos subduction zone. For both events, velocity P and SH waves recorded at teleseismic distances were modeled. For the 1989 San Marcos event, two slip zones were determined with a maximum slip of 121cm, a stress drop of 8bars and a rupture duration of approximately 13s. This event showed a complex rupture. For the 2021 Acapulco event, a zone of maximum slip of 267cm, a stress drop of 5bars, and a rupture duration of approximately 24s were determined. Analysis of rupture zones suggests that complex events occur in the Acapulco–San Marcos subduction zone. Therefore, these results have important implications in seismic potential studies since the source parameters are critical.

KEYWORDS **Interplate earthquake. Slip models. Rupture zone. Cocos plate.**

INTRODUCTION

In the Guerrero region, the Cocos plate subducts below the North American plate (Pardo and Suárez, 1995; Pérez-Campos *et al*., 2008). This process has generated several large earthquakes in the interplate contact zone updip of the flat slab region. The largest events that have occurred in this zone since 1890 are the 1899 event (Ms 7.9) that probably covered the entire Guerrero Gap zone according to Ortiz *et al.* (2000), the event of April 15, 1907 (Ms 7.9), and the earthquake of July 28, 1957 (Ms 7.8). The 1962 doublet (Mw 6.9; 7.0) also occurred in this area. According to Nishenko and Singh (1987), the recurrence time in the Guerrero subduction zone is 60–70 years. The 1962 doublet of May 11 and 19 had a simple and a complex rupture, respectively (Singh and Mortera, 1991).

Ortiz *et al.* (2000) determined the location and dimensions of the ruptures of the 1962 and 1957 earthquakes, from tsunamis recorded at the tide gauges of Acapulco and Salina Cruz. They located the rupture zones of the 1962 events primarily inland to the NW and SE of Acapulco. For the earthquake of July 28, 1957, the results indicate that the northeast limit of the rupture is located 30km southeast of Acapulco with a length of 90km (Ortiz *et al*., 2000). The 1989 San Marcos (Mw 6.9) and 2021 Acapulco (Mw 7.0) earthquakes occurred in the Acapulco–San Marcos region.

The 1989 Guerrero earthquake is the most recent event of large magnitude that has occurred in the San Marcos area since 1957. Zuñiga *et al.* (1993) determined an aftershock area of 780km^2. The aftershock area overlaps with of the 1957 event (Zuñiga *et al*., 1993). The San Marcos event had a high spectral level of 0.2 and 0.6Hz (UNAM Seismology Group, 2015).

On September 8, 2021 the Acapulco event (Mw 7.0) occurred off the coast of Guerrero, Mexico, west of the Guerrero gap. The last event that ruptured in the Guerrero gap was on December 16, 1911 (Mw 7.6). The 2021 event occurred near the 1962 doublet of May 11 and May 19 (Nishenko and Singh, 1987; Ortiz *et al*., 2000). These 1962 earthquakes generated small tsunamis and neither of the two events caused damage (Merino *et al*., 1962; Ortiz *et al*., 2000). Recently, Melgar *et al.* (2022) determined a slip model of the Acapulco 2021 event using strong motion, GNSS (Global Navigation Satellite System), tide gauge and InSAR (Interferometric Synthetic Aperture Radar) data. They determined that two asperities broke in this event. Gonzalez-Huizar (2021) mentions that fewer aftershocks of the 2021 event occurred within the Guerrero seismic gap than on the opposite side of the epicenter, outside the gap.

In the study area, the Cocos plate subducts under the North American plate with a convergence rate of 4cm/yr (DeMets *et al*., 1997). Nishenko and Singh (1987), Suarez *et al.* (1990) and Singh and Mortera (1991) have suggested the possibility that the entire region from -101.2 to -99.1 longitude could break in a single event of magnitude Mw>8.0. Figure 1 shows the earthquakes with Mw≥ 6.9 that have occurred

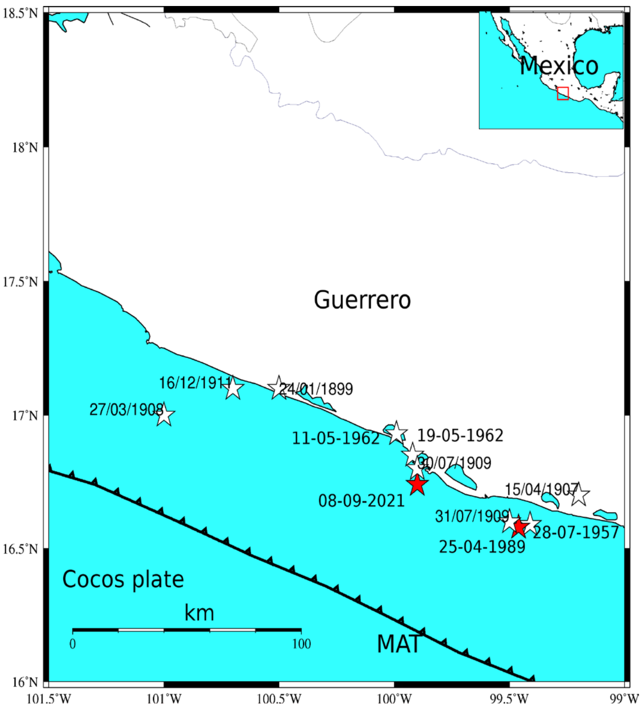

FIGURE 1. Epicentral locations (stars) of Mw≥6.9 events that have occurred from 1899 to date in the Guerrero subduction zone that includes the Acapulco–San Marcos region, Guerrero. MAT is Mesoamerican Trench.

in the Guerrero region in the last 130 years (Table 1). The last events in the Acapulco–San Marcos region are the 1989 event and the 2021 event. The San Marcos event of 1989 and the Acapulco event of 2021 have digital data available, and their rupture models can be determined to understand the behavior and relationships of interplate earthquakes.

Data

To determine the slip patterns, teleseismic body waves recorded at the global digital stations from the Incorporated Research Institutions for Seismology (IRIS, 2021) were inverted. We use P waves recorded between 25 and 95 degrees and SH waves recorded between 35 and 80 degrees to minimize the effects of core diffraction, upper mantle propagation, and mantle triplications. P waves were obtained from the vertical recordings, and SH waves were recovered by rotating the horizontal components. Records were converted to ground velocities. We use the widest possible bandwidth for observations. For the 1989 event, P waves of broadband, intermediate period and long period records were inverted. Broadband SH records were also used for this event. For the Acapulco 2021 event, P and SH waves of broadband recordings were inverted. For the broadband and intermediate period recordings, we apply a bandpass filter in a period range between 1–60s and resample the waveforms at 0.25s. Long period records were filtered between 10–80s and resampled at 1s. Figure 2 shows the distribution of stations used to generate each slip model. Figure 2A shows the stations for the 1989 San Marcos event, and Figure 2B shows the stations for the 2021 Acapulco event.

METHODS

We used the method developed by Hartzell and Heaton (1983; 1986) which has been used in the subduction zone

TABLE 1. Interplate earthquakes (Mw≥6.9) that have occurred in the Guerrero subduction zone (98.5oW- 100.0oW)

Event (year/month/day)	Latitude (°)	Longitude(°)	Magnitude
17/01/1899	17.10	-100.5[1]	Ms7.5
15/04/1907	16.62	-99.22[1]	Ms 7.9
26/03/1908	16.30	-98.50[1]	Ms 7.8
30/07/1909	16.80	-99.90[2]	Ms 7.5[5]
31/07/1909	16.62	-99.45[2]	Ms 7.1
16/12/1911	17.00	-100.70[2]	Ms 7.6
28/07/1957	16.76	-99.35[3]	Ms 7.8
11/05/1962	16.93	-99.99[2]	Ms 7.1
19/05/1962	16.85	-99.92[2]	Ms 7.0
25/04/1989	16.58	-99.46[4]	Mw 6.9
08/09/2021	16.78	-99.93[5]	Mw 7.0

*Numbers shown as superscripts indicate references: 1 Anderson *et al.* (1989), 2 Santoyo *et al.* (2005), 3 Gonzalez-Ruiz and McNally (1988), 4 Zuñiga *et al.* (1993), 5 SSN catalog.

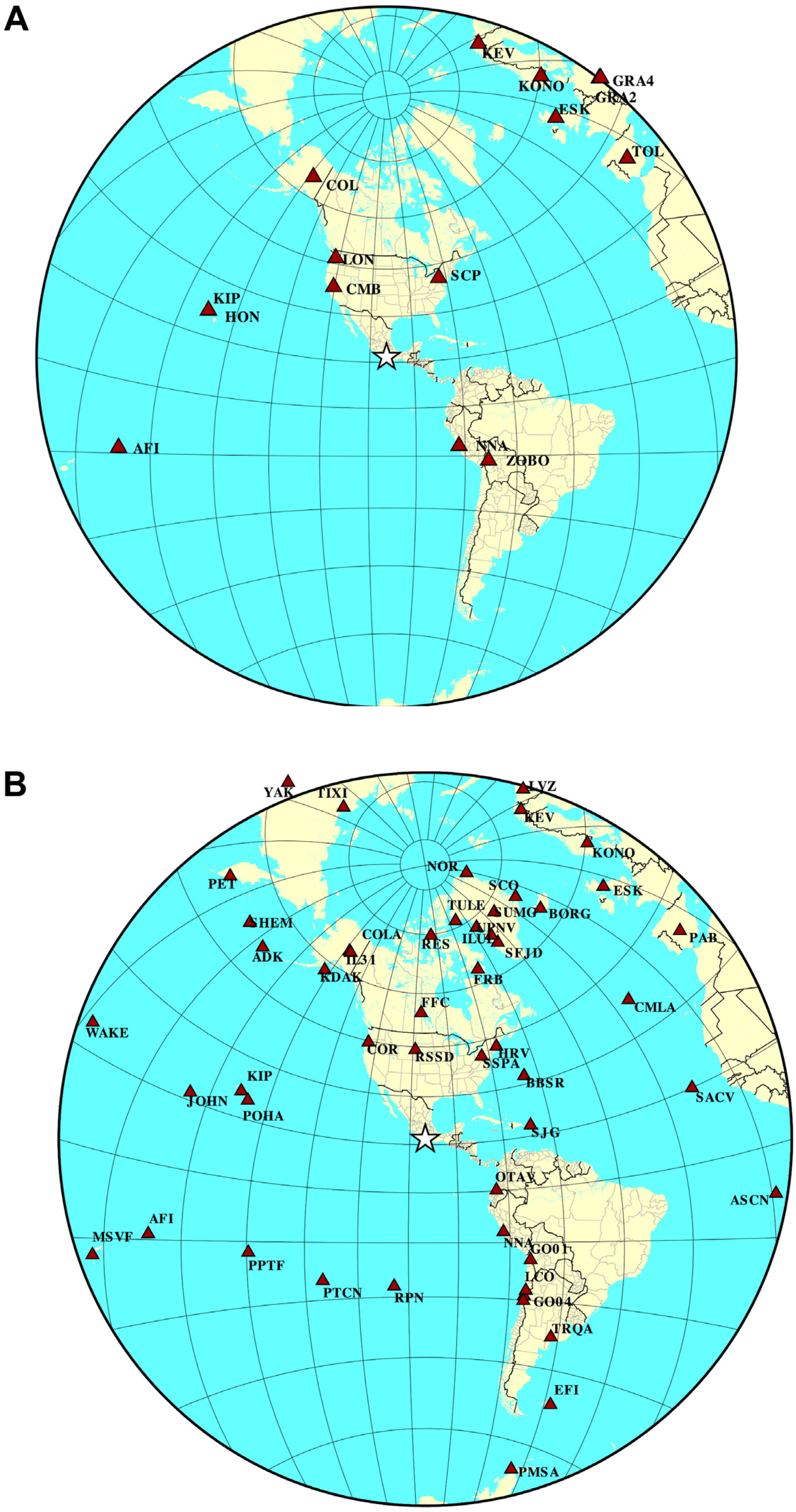

FIGURE 2. Azimuthal distribution of seismic stations used in the kinematic inversion of the events of: A) San Marcos 1989 and B) Acapulco 2021. The stars represent the epicenter. The triangles represent the location of the stations.

of the Mexican Pacific coast (*e.g.* Martínez-López and Mendoza, 2018; Mendoza, 1993, 1995; Mendoza and Hartzell, 1988, 1999; Mendoza and Martínez-López, 2017). It is based on a kinematic parameterization of the fault to identify the coseismic slip distribution that best reproduces the recorded waveforms. A fault plane with orientation and geometry based on the focal mechanism of the earthquake is identified. The fault is subdivided into a specific number of cells, and the location of the hypocenter is fixed. Synthetic seismograms are calculated for each subfault assuming that each of these is composed of point sources uniformly distributed across the subfault dimensions. Each of the point sources is assumed to trigger when the rupture front, traveling at a constant velocity along the fault from the hypocenter, reaches that point. The responses for each point source are calculated using a fixed duration boxcar function and a crustal model. Each point source is delayed by the rupture time and summed to obtain the synthetic seismogram for each subfault.

The inversion problem is linear and constructed by putting the seismograms generated for each subfault of all stations one after another to form the columns of a matrix of synthetic amplitudes. The number of columns then corresponds to the number of subfaults considered in the inversion. The waveforms observed at all stations are similarly put together one after another to form a data vector. Details of the methodology can be seen in Hartzell and Heaton (1983, 1986). To allow flexibility in the rupture start time in each subfault, additional columns are added to the coefficient matrix where the synthetics in each subfault are delayed by the width of the rectangular function that was used to generate the Green's functions. The number of times that the synthetics of each subfaults are delayed and added to the coefficient matrix corresponds to the number of time windows used to discretize the duration of the dislocation.

To determine the uncertainties in the slip models due to possible errors in the fault geometry (strike, dip, rake), focal depth and rupture velocity, a simple sampling procedure similar to that used by Hartzell *et al.* (2013) and Martínez-López and Mendoza (2018) was used, which consists in randomly varying certain input parameters. Random errors in the focal mechanism, depth and rupture velocity were considered in this study. The random numbers are uniformly distributed. In order to identify the range of error for these input parameters, several tests were carried out. The tests consisted of first varying the geometry of the fault by 10º and plotting the residuals of the Euclidean Norm, in addition to visually eviewing the output of the models.

The velocity models of Stolte *et al.* (1986), Suárez *et al.* (1992) and Domínguez *et al.* (2006) were analyzed to determine the velocity model that best fit the data. Each of those velocity models were tested. Table 2 gives estimates of the misfit between observed and synthetic measures of the Euclidean norm ||Ax-b|| and shows that the lowest value was obtained with the velocity model of Suárez *et al.* (1992), which is used in this study.

SLIP MODEL OF SAN MARCOS EARTHQUAKE OF APRIL 25, 1989

Table 3 shows the known source parameters for the 1989 San Marcos event. For this event, 22 P waves and 3 SH waves were inverted. To generate the slip model for the San Marcos event (Mw 6.9), several tests were performed using depths between 10 and 20km corresponding to the depths reported by different researchers and seismic networks. These tests showed that the hypocentral depth that best fit the data is 15km. Dimensions of 60x60km were used, where it was

TABLE 2. Inversion results for different crustal models

Velocity Model	Euclidean Norm (||Ax-b||)
Stolte *et al.* (1986)	11.046
Suárez *et al.* (1992)	10.710
Domínguez *et al.* (2006)	10.795

TABLE 3. Parameters of the source of the earthquake of April 25, 1989, in San Marcos, Guerrero, Mexico

Latitude	Longitude	*H (km)	Mechanism strike, dip, rake(º)	Mw	Reference
16.80	-99.28	23.0			SSN
16.77	-99.33	19.2			NEIC
			276, 10, 66	6.9	Global CMT Project
16.77	-99.32	15.5	255, 29, 51		Pacheco *et al.*, 1993
16.77	-99.27	24.1			Engdahl *et al.*, 1998.
16.58	-99.46	17.3			Singh and Ordaz, 1994

*H=Depth

observed that the rupture zone did not cover the entire fault. Thus, fault dimensions of 48x48km were used with a subfault size of 3x3km. In total, 256 subfaults were used. A rupture velocity of 2.7km/s was used, since this rupture velocity has been used to generate prior slip models for Ometepec, Guerrero (Mendoza and Martínez-López, 2021). The model was generated using the Global CMT (Centroid Moment Tensor). Project focal mechanism and the focal mechanism reported by Pacheco *et al.* (1993), and we found that the data fit better with the focal mechanism reported by the Global CMT project. Records were tapered at 30s and 35s after the start of the broadband and long period recordings, respectively, to minimize non-source propagation effects (Martínez-López and Mendoza, 2018). A record length of 50s was inverted. A rise time of 3s was determined for this event following an inversion using ten-time windows with a length of 1s. In addition, several tests were carried out to find the smoothing value that best fit the data.

Figure 3A shows the coseismic slip distribution obtained for the 1989 San Marcos event. For this event, we estimate a total seismic moment of 1.85 e26 dyne-cm, which corresponds to a moment magnitude of Mw 6.8 (Figure 3B). The moment-rate function was calculated for the event, where it is observed that most of the energy was released during the first 8s. Also, the event had a rupture duration of 13s (Figure 4A).

The parameters were determined following Somerville *et al.* (1999) to determine the rupture zone (Table 4). A rupture zone of 1400km², an average slip of 30cm, and a stress drop of 8bars were obtained (Table 4). In the slip model, a zone of maximum slip is observed for the San Marcos event of 1989 that extends into the down-dip area. Another zone of maximum slip is also observed to the southeast of the hypocenter. This suggests that perhaps the event broke two asperities. In this work, it is observed that the event of San Marcos 1989 was not a simple event as other researchers have proposed (*e.g.* Santoyo, 1994).

SLIP MODEL OF ACAPULCO EARTHQUAKE OF SEPTEMBER 8, 2021

The slip model of the 2021 Acapulco event was determined using teleseismic P and SH waves in velocity.

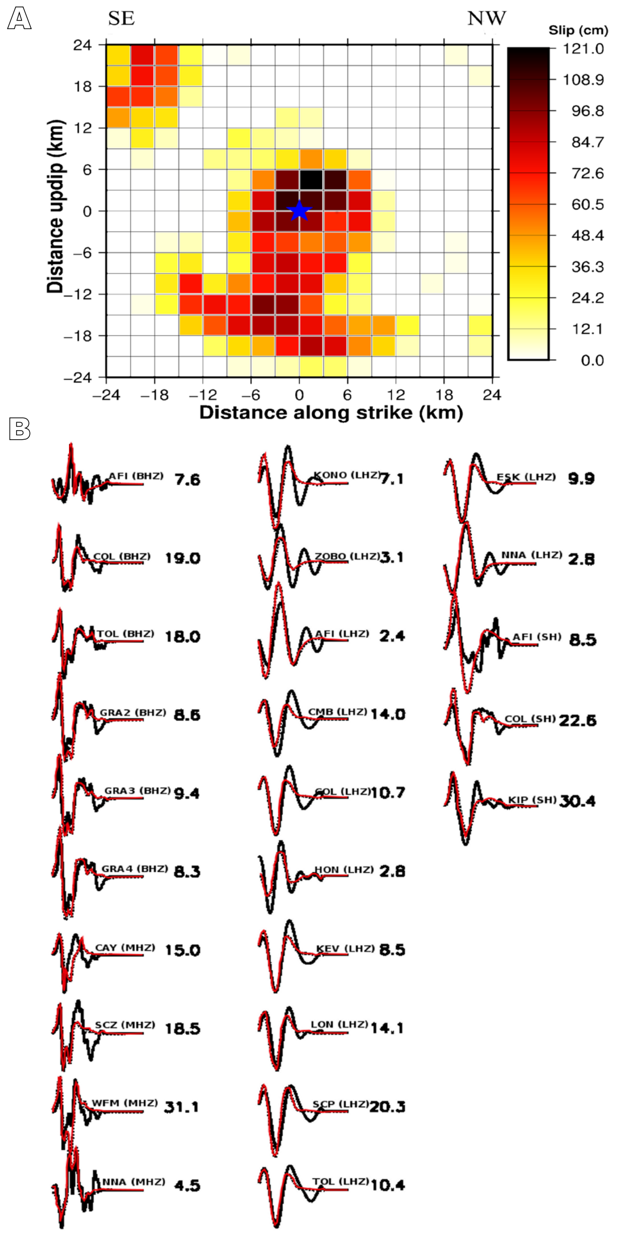

FIGURE 3. A) Slip distribution obtained for the San Marcos 1989 event from the inversion of P (Primary) and SH (Horizontal Shear) wave teleseismic data. B) Fits between observed (solid line) and synthetic (red line) data to obtain a seismic moment of 1.85 x 10^{26}dyne-cm (Mw 6.8).

TABLE 4. Properties of the rupture zones of the San Marcos 1989 (Mw 6.9) and Acapulco 2021 (Mw 7.1) events

Event	Area (km²)	Mo (dyne-cm)	Slipmean (cm)	Slipmax (cm)	Stress drop (bar)
25-Apr-1989	1400km²	1.87e26	30	121	8.0
08-Sep-2021	1750km²	5.75e26	37	267	5.0

Table 5 shows the source parameters of the 2021 event. A total of 49 records were inverted, of which 36 correspond to P waves and 13 SH waves. Tests were made considering a filter from 0.5 to 60s, however the result obtained is very similar when using a filter from 1 to 60s. Therefore, a filter from 1 to 60s was used. A record length of 50s was inverted with a taper after 30s and 35s for P and SH waves, respectively. Also, tests were made using different subfault sizes and similar results are observed. Fault dimensions of 80km long and 80km wide were used, divided into 256 subfault of 5kmx5km. After several tests, it was observed that the hypocenter that best fits the data is located at a depth of 15km. The fault plane reported by the Global CMT Project was used because it best fit the observed data. A run was made using ten-time windows of 1s, and it was determined that the rise time corresponding to the event is 3s.

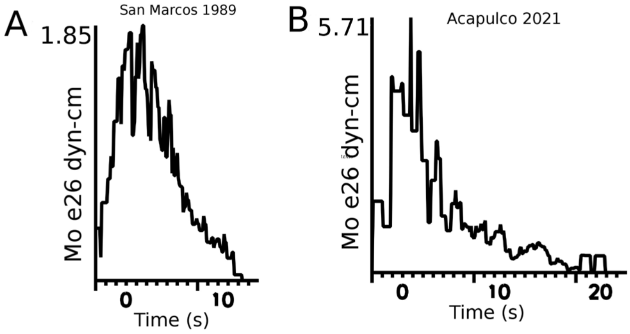

FIGURE 4. A) Moment-rate function for the San Marcos 1989 event obtained for the seismic moment of 5.71 x 10^{26}dyne-cm (Mw 7.1). B) The far field source-time function obtained for the Acapulco 2021 event.

Figure 5A shows the slip distribution obtained for the 2021 event from the inversion of teleseismic data. A zone of high slip is observed in the downdip. Also, slip is observed in the updip zone, but with slip values corresponding to approximately 20% of the maximum slip. Figure 5B shows the slip model fits, corresponding to a seismic moment of 5.7e26dyne-cm (Mw 7.1). Figure 4B shows the moment-rate function of the event, where a source is observed with energy release in the first 2 seconds and the greatest energy release is observed at 8s. The event had a duration of approximately 24s. In addition, the rupture zone was determined following Somerville *et al.* (1999) to the determined slip model. Table 4 lists the properties of the rupture of the 2021 event defined from the model. This event had a maximum slip of 267cm and a stress drop of 5.0bars.

A test was also carried out where the slip model for the 2021 event was determined using the velocity models of Stolte *et al.* (1986), Suárez *et al.* (1992) and of Dominguez *et al.* (2006). The rupture zones for the slip models were defined following Somerville *et al.* (1999). It is observed that the rupture zone of the 2021 event is similar using the velocity models of Suarez *et al.* (1992) and Dominguez *et al.* (2006). However, the rupture length using the model of Stolte *et al.* (1986) is 20km smaller in the strike direction. A similar width was observed in the three slip models.

Uncertainties in slip models

The slip models were determined using data recorded at teleseismic distances that allow identification of areas of high slip. The possible errors in the input parameters were determined from the variability of the input parameters of the geometry of the fault, the depth and the rupture velocity. To determine the uncertainties, 300 independent inversions were run for each event using combinations of the input parameters. Initially, the geometry of the fault was varied at 10º, and it was observed that not all combinations fit the data. In the adjustments there were models in which the data were not well fit, mainly in the arrival of the P wave and in the shape of the wave. Then, a variability of 6º in the geometry of the fault was taken, and it was observed that some models did not fit. Therefore, it was subsequently varied by 5º and it was observed that all the data fit, although there are models that have a better fit. In general, all settings are acceptable. Therefore, the values are varied in a range of ±5º for the fault geometry, ±2km for the depth, and ±0.2km/s for the rupture velocity. This implies that all those models with a variability of ±5º in the

TABLE 5. Parameters of the source of the event of September 8, 2021 (Mw 7.0)

Latitude	Longitude	Depth (km)	Mechanism strike, dip, rake (º)	Mw	Reference
17.12	-99.60	30			Huang *et al.*, 2021
16.98	-99.77				Perez-Oregon *et al.*, 2021
16.78	-99.93	10	288, 13, 89	7.1	SSN
16.97	-99.93	20	275, 21, 76	7.0	USGS
			277, 21, 71	7.0	Global CMT Project

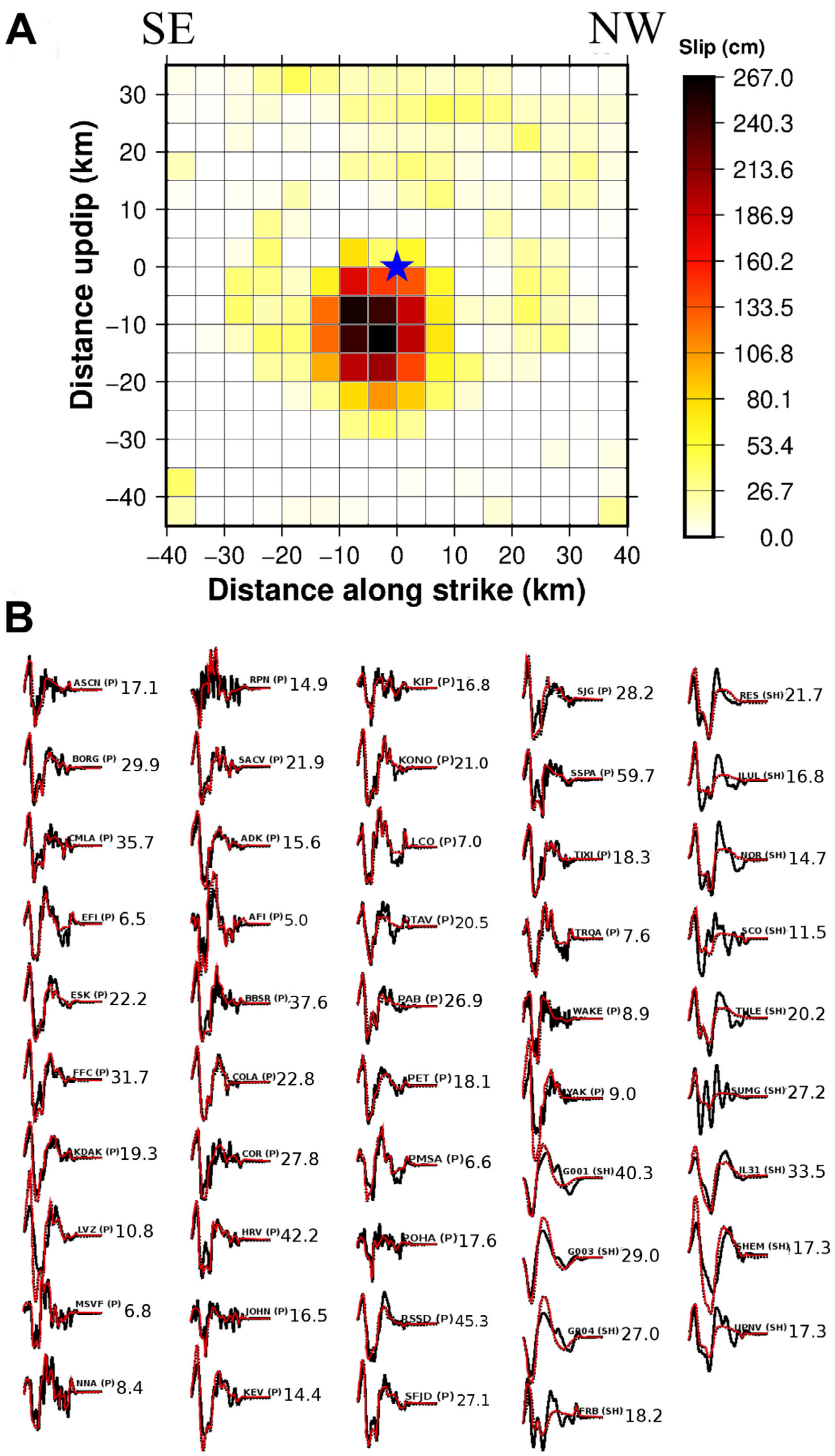

FIGURE 5. A) Slip distribution inferred for the 2021 Acapulco event from inversion of broadband teleseismic records. B) Fits between the observed (solid line) and synthetic (red line) data for the P (Primary) and SH (Horizontal Shear) wave recordings. The number at the end of each record indicates the maximum amplitude of the record.

fault geometry, ±2km in depth and ±0.2km/s in the rupture velocity are possible solutions of the model.

Figure 6A shows the average, the standard deviation (Figure 6B), and the coefficient of variation of the slip observed for each subfault for the San Marcos event (Figure 6C). On average, it is observed that the area corresponding to the rupture zone is very similar to the model obtained for the San Marcos 1989 event (Figure 6A). For the standard deviation it is observed that the largest values are found in the zones of maximum slip (Figure 6B). There is also an area of what in the upper left part of the model. The coefficient of variation of the slip model ranges from 30% to 60% (Figure 6C). However, in the down-dip zone a variation of 10 to 20% is observed. Regarding the slip zone that is located in the upper left part of the hypocenter, the variabilities in recovered slip is between 60 and 80%, which suggests that this zone is not well defined, and the resolution of the data does not allow us to suggest whether it is an asperity.

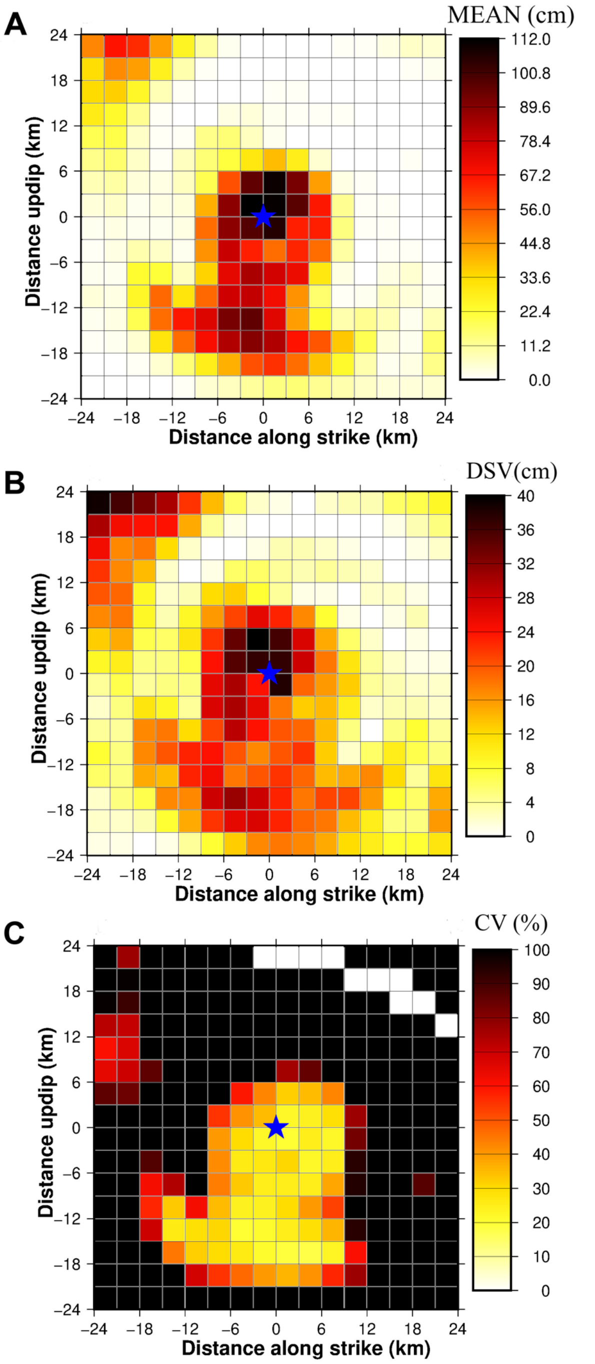

FIGURE 6. A) Average slip in each subfault of the 300 independent inversions for the San Marcos event. B) Slip standard deviation (centimeters) estimated for each subfault after 300 independent inversions varying fault geometry, depth and rupture velocity. C) Slip variation coefficient in each subfault of the 300 inversions.

Figure 7 shows the uncertainties of the slip model of the 2021 Acapulco event. Figure 7A shows the mean of the 300 inversions of the event, and it is observed that is similar to the slip model obtained in Figure 5A. In the standard deviation plot, high slip zones are observed where the high slip zone is located and high slip values to the east of the hypocenter (Figure 7B). Also, slip is observed in the updip area (Figure 7B). Figure 7B shows that in the 300 inversions, we have solutions with two zones of maximum slip. The 300 solutions were reviewed and some of the models were found to have two zones of maximum slip, one in the updip direction and another one with the largest slip in the downdip area. Also, we have solutions that have two source zones, a small one to the southeast of the hypocenter and another near the hypocenter. This suggests that there are some models with more than one high slip zone that show complexity not observed in Figure 5A. This is due to the limited resolution of the teleseismic data, where it is more appropriate to determine the slip model from a joint inversion of local, regional and teleseismic data. Figure 7C shows that the coefficient of variation is mainly between 10% and 40%. However, the area where the maximum slip (seen in Figure 5A) is found has a variability of 10%. This suggests that this area is well defined in terms of location and size. The uncertainty in the slip model of the 2021 event was also reviewed using the crustal velocity models of Stolte *et al.* (1986), Suárez *et al.* (1992) and Domínguez *et al.* (2006). More than 300 independent inversions were run varying the fault geometry (±5º), the depth (±2km), and the rupture velocity (±0.2km/s). In the analysis of the coefficient of variation, a minor uncertainty is observed using the crustal model of Suárez *et al.* (1992), although the uncertainty is similar to that defined with the velocity model of Domínguez *et al.* (2006).

Interplate earthquakes in Acapulco – San Marcos

Figure 8A shows the aftershock areas of the large earthquakes of May 11 and May 19, 1962, July 28,

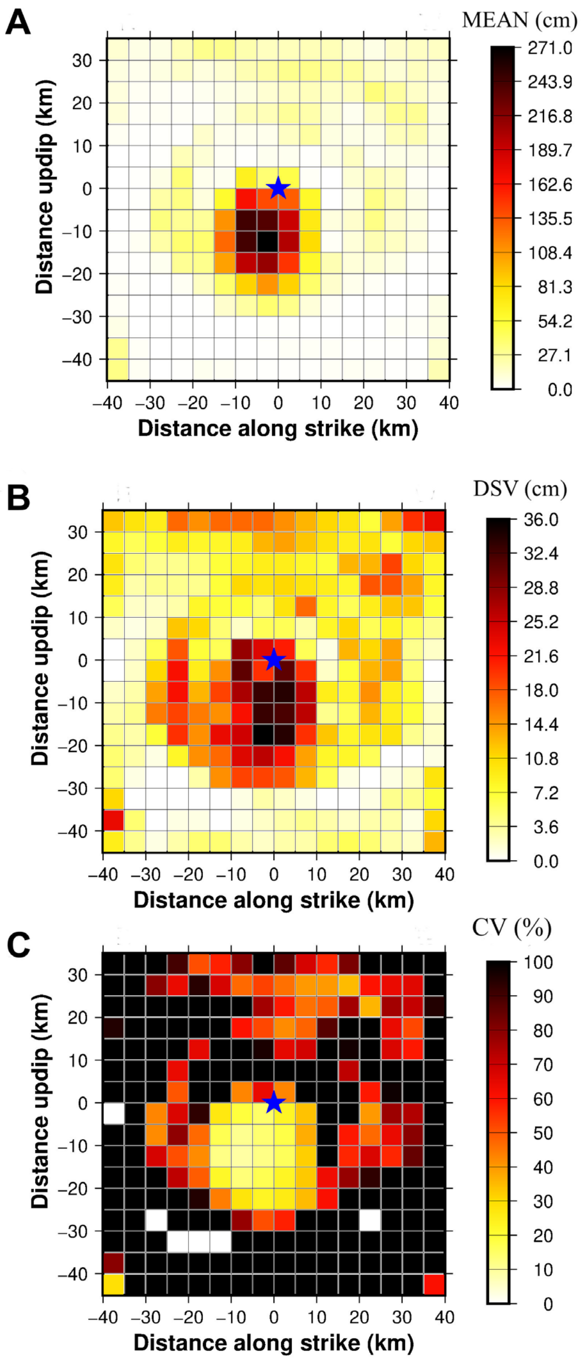

FIGURE 7. A) Average slip in each subfault of the 300 independent inversions for the San Marcos event. B) Slip standard deviation (centimeters) estimated for each subfault after 300 independent inversions varying fault geometry, depth and rupture velocity. C) Slip variation coefficient in each subfault of the 300 inversions.

1957, April 25, 1989, and the distribution of Mw≥ 3.8 aftershocks of the 2021 event located during the first 10 days by the National Seismological Service (SSN) of Mexico. It is observed that the aftershock zones of the 2021 event overlap with the aftershock zones of the 1962 event. Also, it is observed that the aftershock areas of the 2021 and 1962 event partially overlap with the aftershocks of the 1957 event. Figure 8B shows the rupture zones of the events of May 11, 1962, May 19, 1962, July 28, 1957, April 25, 1989 and September 8, 2021. In this figure, it is observed that the rupture zone of the 2021 Acapulco event overlaps with the ruptures of the 1962 events. Also, the rupture zone of the 1989 event is within the rupture zone of the 1957 earthquake as observed in the areas of aftershocks. In addition, it is observed that the rupture zones of the 1957 event do not overlap with the rupture zones of the second event of 1962 and the 2021 earthquake. Therefore, the 2021 Acapulco event did not cover the rupture zone of the 1957 Acapulco event.

The slip model of the 1989 event suggests that it is a complex event. The source function of the 1957 event determined by Singh and Mortera (1991) also suggests that it was a complex event. This suggests that complex events occur in the San Marcos region. The 1957 event caused immense damage in Mexico City, so it is important to study the earthquakes that occur in this area. In the San Marcos region, no other event has occurred since the 1989 earthquake, although this earthquake had a magnitude of Mw 6.9, approximately 0.8 times less than the magnitude of the 1957 event. As far as the Acapulco region is concerned, the 2021 event is the last event of magnitude greater than or equal to 7.0 to have occurred east of the Guerrero Gap.

On the other hand, Iglesias *et al.* (2022) compares the seismograms of the May 11, 1962 event with the 2021 event, and they suggest that the 2021 event is a repeat of the May 11, 1962 event. Our results suggest that the rupture zone of the 2021 event and that of the 1962 events are overlapping. The asperity defined in the downdip region of the fault overlaps with the rupture zone defined for the event of May 11, 1962. However, the rupture zone defined in this work extends to the northwest of the hypocenter and therefore covers the rupture zones of the two 1962 events, although a high slip zone is not observed on the northwest side of the rupture area.

The 1907 event (Ms 8.0) occurred in this area and the rupture was 110–140km long (Nishenko and Singh, 1987). Therefore, this region of Acapulco–San Marcos could perhaps break in a single event that could have downdip dimensions of approximately 125km and a segment length of approximately 140km if we consider the seismogenic width recently determined by Martinez-Lopez *et al.* (2022). This corresponds to an event of magnitude Mw 8.0 if we apply the equation of Murotani *et al.* (2013).

DISCUSSION

Large earthquakes have occurred in the Acapulco–San Marcos area, generated by the interaction of the North

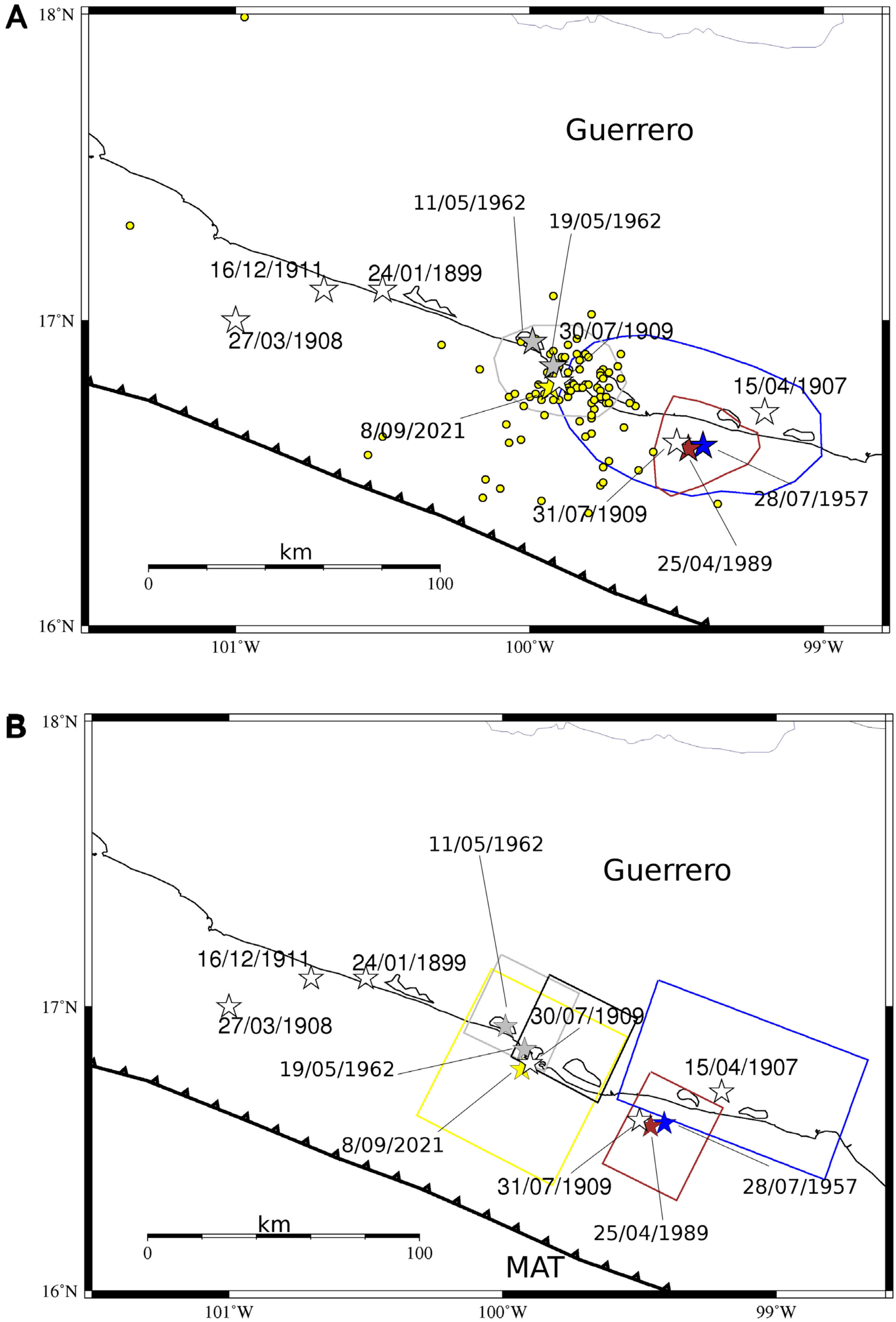

FIGURE 8. A) The aftershock zones of the events of May 11 and 19, 1962 (Mw 6.9; 7.0), July 28, 1957 (Ms 7.8), April 25, 1989 (Mw 6.9) and the distribution of aftershocks of the event of September 8, 2021 (Mw 7.0) obtained by the SSN during the first 10 days following the event. B) Rupture zones defined by applying the procedure of Somerville *et al.* (1999) for the San Marcos 1989 and Acapulco 2021 events. Also shown are the rupture zones of the 1962 and 1957 events determined by Ortiz *et al.* (2000).

American and Cocos plates. The events of San Marcos in 1989 and Acapulco in 2021 occurred in this region. The rupture model of the 1989 San Marcos event shows two zones of maximum slip. The rupture zone determined in this study is larger than the aftershock zone determined by Zuñiga *et al.* (1993). The stress drop determined for this event is less than 10bars. This value is consistent with the stress drop observed for interplate events in seismogenic coupling zones (Allmann and Shearer, 2009; Martínez-López and Mendoza, 2018). The drop stress determined for the 2021 Acapulco event is consistent with the values obtained for the 1982 doublet occurred in Ometepec, Guerrero (Astiz and Kanamori, 1984). This suggests that in the region where doublets occur the stress drops are minor, about equal to 5bars.

The analysis of the crustal velocity model for the determination of the slip model of the 2021 event does not significantly affect the derivation of the zone of maximum slip defined with teleseismic data. However, the 2021 rupture zone seems to be affected using the velocity model of Stolte *et al.* (1986). The length of the rupture zone defined using the velocity model of Stolte *et al.* (1986) is 20km smaller in comparison to the rupture zones defined with the models of Suárez *et al.* (1992) and Domínguez *et al.* (2006). However, the rupture width did not vary using different velocity models. This could suggest that the velocity model affects the rupture length defined for the event but does not affect the zone of maximum slip and width of the rupture zone defined using teleseismic data.

From the analysis of the uncertainties of the 300 independent runs using different velocity models, it was possible to observe that in general the velocity model does not significantly affect the zone of maximum defined slip. However, a more detailed evaluation is necessary to quantitatively determine how the velocity model affects the coseismic slip distribution. This analysis is outside the scope of this study.

The slip model of the 2021 event was also determined by Melgar *et al.* (2022) using strong motion, GNSS, tide gauge, and InSAR data. In the slip model determined by Melgar *et al.* (2022), two maximum slip zones are observed: a zone of maximum slip in the downdip portion of the rupture zone and another in the updip part. In the model determined in this study, a zone of maximum slip is observed in the downdip zone and slip corresponding to approximately 20% of the maximum slip is observed in the updip area. Therefore, slip above and below the hypocenter is observed. However, in our model two asperities are not observed, this could be due to the resolution of the data. However, in the 300 independent runs there are models that have slip values in the updip zone that correspond to 45% of the maximum slip. Melgar *et al.* (2022) determine an asperity in the updip zone that corresponds to approximately 40% of their maximum slip. On the other hand, the slip model determined here with teleseismic data defines an asperity in the downdip region of the fault, which is consistent with the source zone defined by Melgar *et al.* (2022). However, Melgar *et al.* (2022) determine a second asperity in the updip area. Our data do not allow this second asperity to be defined, but the defined slip model for 2021 shows slip updip. Although the uncertainty analysis suggests that more than one asperity may have broken, it is observed that some runs have high slip in the updip area and southeast of the hypocenter. Therefore, the uncertainty analysis allows us to observe that more than one asperity broke for the 2021 event. However, for a detailed study of the properties of asperities for this event it is necessary to carry out a joint inversion of local data, regional and teleseismic.

Also, in Figure 9 the aftershock zones of the 2021 event are observed updip and downdip of the hypocenter, consistent with the determined rupture zone in this study. Gaps are observed between the aftershocks. It has been observed that aftershocks are located outside asperity zones (*e.g.* Mendoza and Hartzell, 1988), suggesting that perhaps an asperity may have broken in those gaps where aftershocks are not observed. Also, in Figure 9 it is observed that in general the aftershock areas are smaller than the defined rupture zones of the waveform inversion. However, it would be useful to carry out a detailed study of the rupture and aftershock zones to know how they compare with each other.

Also, in Figure 8B the events have ruptured adjacent regions and there are spaces that have not ruptured in the last 100 years, as has been observed in the Oaxaca subduction zone (Mendoza and Martínez-López, 2021). This suggests that the Guerrero subduction zone has been broken in parts and that another event could occur in the spaces that remain between each event. This is consistent with what Mendoza and Martínez-López (2017) observed in the Michoacan region and east of the Guerrero gap.

The standard deviation analysis of the events that have occurred in the Acapulco–San Marcos area suggests that complex events occur in this region. Therefore, it cannot be ruled out that an event could occur that breaks the entire Acapulco–San Marcos segment. This variable rupture mode has been observed in other subduction zones such as the 2011 Japan event (Mw 9.0) where the plate interface had ruptured in smaller events and a mega-earthquake was not expected (Simons *et al.*, 2011). Therefore, if we consider the seismogenic width of 125km (Martínez-López *et al.*, 2022) and the length of the Acapulco–San Marcos segment, an earthquake of Mw 8.1 could be generated in the study area. The earthquake of September 19, 1985 (Mw 8.1) was located

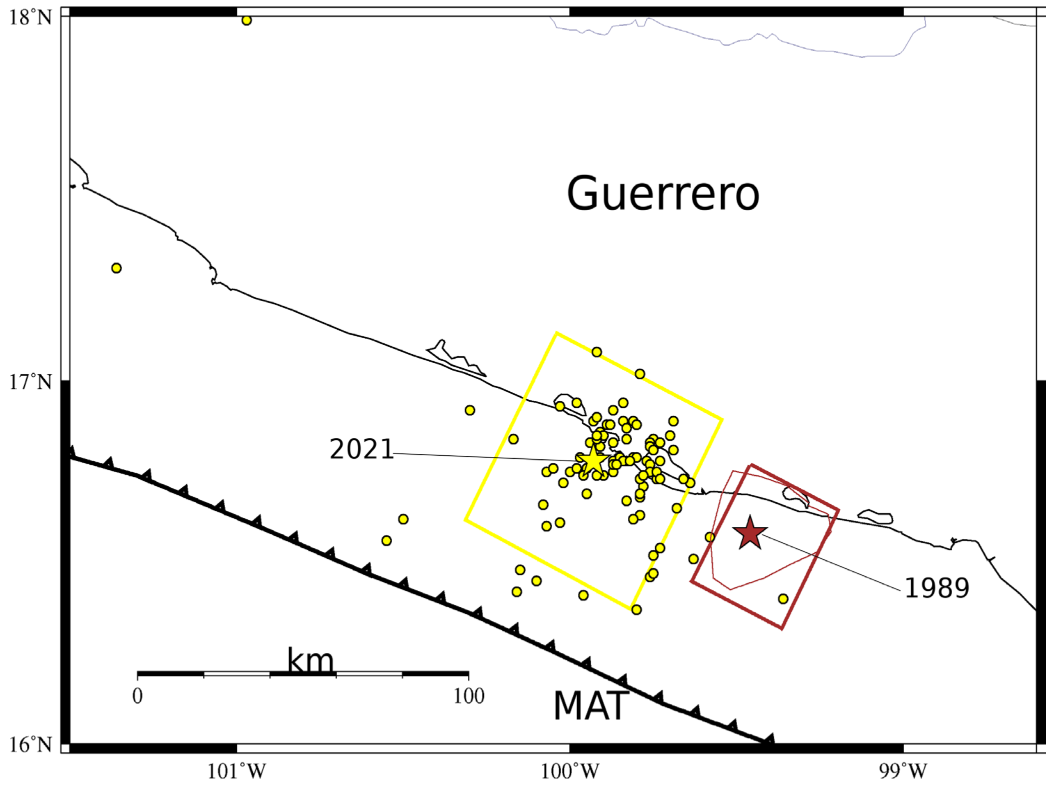

FIGURE 9. Comparison of the 1989 and 2021 rupture zones with aftershock area and aftershock distribution, respectively. The yellow circles represent the Mw≥ 3.8 aftershocks of the 2021 event located by the SSN during the first 10 days following the event. The rectangles represent the rupture zones. The polygon represents the aftershock area of 1989.

almost 400km away from Mexico City (Esteva, 1988). However, the damage caused in Mexico City was immense and constitutes the worst seismic disaster in the history of Mexico (Esteva, 1988). The Acapulco–San Marcos region is approximately 300km distance from Mexico City. Therefore, an earthquake of magnitude 8.1 would cause immense damage to the capital of the country.

Complex rupture events that occur in subduction zones have a major effect on the local tsunami (Geist, 2002). On the other hand, Mueller *et al.* (2015) mention that the complexity of the rupture has a first-order effect on the extent of the inundation for local tsunami sources. Analysis of the standard deviation of the San Marcos (Mw 6.9) and Acapulco (Mw 7.0) events suggests a complex rupture. Hence, these results have implications for the possible scenarios of seismic hazard studies in the Acapulco–San Marcos subduction zone, Guerrero.

Our examination of the uncertainties of the slip models suggests that in general the rupture zone can be recovered from teleseismic data because, on average, the 300 independent models show a similar rupture area. Also, it is observed that there are variations in the slip values in each subfault. We observe a greater uncertainty in the model of the San Marcos event due to the decreased azimuthal coverage, unlike the Acapulco event of 2021. Also, in general, it is observed that the events that have a magnitude of Mw 6.9 to 7.1 have a rise time of about 3s. This is consistent with what Martínez-López and Mendoza (2018) have observed. This information would be useful for quick, real-time slip model determination studies.

CONCLUSIONS

In this work, slip models of the 1989 San Marcos (Mw 6.9) and 2021 Acapulco (Mw 7.1) events were determined from the inversion of P and SH waves from teleseismic records in ground velocity. For the San Marcos 1989 event, two maximum slip zones are observed. This event had a maximum slip of 121cm, a rupture duration of approximately 13s, and a stress drop of 8bars. In addition, it was observed that the 1989 San Marcos event was complex with more than one high slip zone.

For the Acapulco 2021 event, there is a rupture zone that shows a maximum slip of 267cm, a stress drop of 5bars, and a rupture duration of approximately 23s. The moment-rate function suggests that the greatest release of energy occurs in the first 8s. The rupture zone overlaps the rupture zones of the 1962 events defined by Ortiz *et al.* (2000). The uncertainty analysis suggests that more than one asperity could have broken in this event, as other authors have suggested.

In general, the results obtained in this work suggest that the events that occur in the Acapulco–San Marcos subduction zone could be complex. Therefore, it is important to analyze earthquakes in this area because the events that occur in the region could generate damage to Mexico City due to its proximity. If the Acapulco–San Marcos segment was to rupture in a single event, an earthquake of Mw 8.1 could be generated. Therefore, these results have important implications in seismic potential studies since the source parameters are critical.

ACKNOWLEDGMENTS

This research was financed by a DGAPA-UNAM postdoctoral grant and a CONAHCYT postdoctoral scholarship. The author would like to thank Thorne Lay and an anonymous reviewer for constructive comments that improved the manuscript. Carlos Mendoza also provided comments on this work. The images were made with the GMT (Generic Mapping Tools) program by Wessel and Smith (1991).

REFERENCES

Allmann, B.P., Shearer P.M., 2009. Global variations of stress drop for moderate to large earthquake. Journal of Geophysical Research, 114, b01310.

Anderson, J.G., Singh, S.K., Espíndola, J.M., Yamamoto, J., 1989. Seismic strain release in the mexican subduction thrust. Physics Earth Planet Interiors, 58, 307-332.

Astiz, L., Kanamori, H., 1984. An earthquake doublet in Ometepec, Guerrero, Mexico. Physics Earth Planetary Interiors, 34, 24-45.

DeMets, C., Wilson, D.S., 1997. Relative motions of the Pacific, Rivera, North American, and Cocos plate since 0.78Ma. Journal Geophysics Research, 102, B2, 2789-2806.

Domínguez, J., Suárez, G., Comte, D., Quintanar, L., 2006. Seismic velocity structure of the Guerrero gap, Mexico. Geofísica Internacional, 45(2), 129-139.

Engdahl, E.R., Hilst, V., Buland, R.D., 1998. Global teleseismic earthquake relocation with improved travel times and procedures for depth determination. Bulletin Seismological Society of America, 88, 722-743.

Esteva, L., 1988. The Mexico earthquake of September 19, 1985 consequences, lessons, and impact on research and practice. Earthquake Spectra, 4,3, 413-426.

Geist, E.L., 2002. Complex earthquake rupture and local tsunamis. Journal of Geophysical Research, 17, B5, 2086.

González-Huizar, H., Pérez-Campos, X., Velasco, A.A., 2021. Acapulco earthquake struck the edge of a seismic gap. Temblor, 4, DOI: http://doi.org/10.32858/temblor.218

González-Ruiz, J.R., McNally, K.C., 1988. Stress accumulation and release since 1882 in Ometepec, Guerrero, Mexico: Implications for failure mechanisms and risk assessments of a seismic gap. Journal of Geophysical Research: Solid Earth, 93, B6, 6297-6317.

Hartzell, S.H., Heaton, T., 1983. Inversion of strong motion and telesismic waveform data for 478 the fault rupture history of the 1979 Imperial Valley, California, earthquake. Bulletin Seismological Society America, 73, 6A, 1553-1583.

Hartzell, S.H., Heaton, T., 1986. Rupture history of the 1984 Morgan Hill, California, earthquake from the inversion of strong motion records. Bulletin of the Seismological Society of America, 76, 649-674.

Hartzell, S., Mendoza, C., Zeng, Y., 2013. Rupture model of the 2011 Mineral, Virginia, earthquake from teleseismic and regional waveforms. Geophysical Research Letters, 10, 1-6.

Huang, H., Yan, R., Dapeng, L., Song, X., Jian, L., Feng, G., Huang, J., Zeren, Z., Xuhui, Sh., 2021. The variations of plasma density recorded by CSES-1 satellite possibly related to Mexico Ms 7.1 earthquake on 8th September 2021, Natural Hazards Research, 2, 1, 11-16, ISSN 2666-5921, DOI: https://doi.org/10.1016/j.nhres.2021.12.002.

Iglesias, A., Singh, S.K., Castro-Artola, O., Perez-Campos, X., Corona-Fernandez, R.D., Santoyo, M.A., Espíndola, V.H., Arroyo, D., Franco, S.I., 2022. A source study of the Mw 7.0 Acapulco, Mexico, earthquake of 8 September 2021. Seismological Research Letters, 93, 3205-3218.

IRIS, 2021, Incorporated Research Institutions for Seismology available in http://www.iris.edu/, accessed October 2021

Martínez-López, R.M., Mendoza, C., 2018. Caracterización de asperezas de sismos recientes en la zona de subducción de Michoacán-Colima-Jalisco, Mexico. Geofísica Internacional, 57-4, 289-306.

Martínez-López, R.M., Mendoza, C., Iglesias Mendoza, A., 2022. Seismogenic width in the Guerrero-Oaxaca subduction zone Mexico. Journal of South American Earth Sciences, 117, 103885.

Melgar, D., Ruiz-Angulo, A., Crowell, B.W., Jameson Fielding, E., Solano-Hernandez, E.A., 2022. The mechanisms of tsunami amplification and the earthquake source of the 2021 M 7 Acapulco, Mexico, earthquake. Bulletin Seismological Society of America, 112, 2902-2914.

Mendoza, C., 1993. Coseismic slip to two large Mexican earthquakes from teleseismic body waveforms: Implications for asperity interaction in the Michoacán plate boundary segment. Journal Geophysical Research, 98, B5, 8197-8210.

Mendoza, C., 1995. Finite-fault analysis of the 1979 March 14 Petatlan, Mexico, earthquake using telesismic P waveforms. Geophysical Journal International, 121(3), 675-683.

Mendoza, C., Hartzell S., 1988. Afterschock Patterns and main shock faulting. Bulletin of 512 the Seismological Society of America, 78(4), 1438-1449.

Mendoza, C., Hartzell, S., 1999. Fault-slip distribution of the 1995 Colima-Jalisco, Mexico, earthquake. Bulletin of the Seismological Society of America, 89(5), 1338-1344.

Mendoza, C., Martínez-López, M.R., 2017. The Mw 7.3 Papanoa, Mexico earthquake of April 18, 2014: Implications for recurrent Mw> 7 thrust earthquakes in western Guerrero. Geofisica Internacional, 56(1), 13-26.

Mendoza, C., Martínez-López, M.R., 2021. Rupture models of recent Mw> 7 thrust earthquakes in the Guerrero-Oaxaca region of the Mexico subduction zone using teleseismic body waves. Seismological Research Letters, 92(6), 3565-3576. DOI: https://doi.org/10.1785/0220200423

Merino, J., Coronado, Salyano, J., Rosales, E., Martínez M., 1962. Los temblores de Acapulco de 1962, Anal. Instituto. Geofisica, Universidad Nacional Autónoma de México (UNAM), 8, 23-36.

Mueller, C., Power, W., Fraser, S., Wang, X., 2015. Effects of rupture complexity on local tsunami inundation: Implications for probabilistic tsunami hazard assessment by example. Journal Geophysical Research: Solid Earth, 120, 488-502.

Murotani, S., Satake, R., Fujii, Y., 2013. Scaling relations of seismic moment, rupture area, average slip, and asperity size for M~9 subduction-zone earthquakes. Geophysics Research Letters, 40(19), 5070-5074.

Nishenko, S.P., Singh, S.K., 1987. The Acapulco-Ometepec, Mexico, earthquakes of 1907-1982: Evidence for a variable recurrence history. Bulletin of the Seismological Society America, 77, 1359-1367.

Ortiz, O., Singh, S.K., Kostoglodov, V., Pacheco, J., 2000. Sources areas of the Acapulco–San Marcos, Mexico earthquakes of 1962 (M 7.1; 7.0) and 1957 (M 7.7), as constrained by tsunami and uplift records. Geofísica Internacional, 39(4), 337-348.

Pacheco, J.F., Sykes, L.R., Scholz, Ch.H., 1993. Nature of seismic coupling along simple plate boundaries of the subduction type. Journal of Geophysical Research, 98, B8, 14133-14159.

Pardo, M., Suárez, G., 1995. Shape of the subducted Rivera and Cocos plates in southern Mexico: Seismic and tectonic implications. Journal of Geophysical Research, 100(B7), 12357-12373.

Perez-Campos, X., Kin, Y., Husker, A., Davis, P.M., Clayton, R.W., Iglesias, A., Pacheco, J.F., Singh, S.K., Manea, V.C., Gurnis, M., 2008. Horizontal subduction and truncation of the Cocos plate beneath central Mexico. Geophysical Research Letters, 35(18), 118303.

Perez-Oregon, J., Varotsos, P.K., Skordas, E.S., Sarlis, N.V., 2021. Estimating the Epicenter of a future strong earthquake in southern California, Mexico, and Central America by means of natural time analysis and earthquake nowcasting. Entropy, 23, 1658. DOI: https://doi.org/10.3390/e23121658

Santoyo, G.G.M.A., 1994. Estudio del proceso de ruptura del sismo del 25 de septiembre de 1989 usando registros de movimientos fuertes y telesismicos. PhD. Thesis. México, Universidad Nacional Autónoma de México, 69pp.

Santoyo, M.A., Singh, S.K., Mikumo, T., Ordaz, M., 2005, Space-time clustering of large thrust earthquake along the Mexican subduction zone: An evidence of source stress interaction. Bulletin of the Seismological Society of America, 95(5), 1856-1869.

Simons, M., Minson, S.E., Sladen, A., Ortega, F., Jiang, J., Owen, J.S.E., Meng, L., Ampuero, J., Wei, Sh., Chu, R., Helmberger, D.V., Kanamori, H., Hetland, E., Moore, A.W., Webb, F.H., 2011. The 2011 magnitude 9.0 Tohoku-Oki earthquake: Mosaicking the megathrust from seconds to centuries. Science, 332, 1421-1425.

Singh, S.K., Mortera, F., 1991. Source time funtions of large mexican subduction earthquakes, morphology of the Benioff zone, age of the plate, and their Tectonic implications. Journal of Geophysical Research, 96, B13, 21487-21502.

Singh, S.K., Ordaz, M., 1994. Seismic release in Mexican subduction zone earthquakes. Bulletin of the Seismological Society of America, 84(5), 1533-1550.

Somerville, P.K., Irikra, R., Graves, S., Sawada, D., Wald, N., Abrahamson, Y., Iwasaki, T., Kagawa, N., Smith, A., Kowada, A., 1999. Characterizing crustal earthquake slip models for the prediction of strong ground motion. Seismological Research Letters, 70, 59-80.

Stolte C., McNally K.C., González-Ruiz J., Simila G.W., Reyes A., Rebollar C., Munguia L., Mendoza L., 1986. Fine structure of a post-failure wadati-Benioff zone, Geophysical Research Letters, 13, 577-580.

Suárez, G., Monfret, T., Wittlinger, G., David, C., 1990. Geometry of subduction and depth of the seismogenic zone in the Guerrero Gap, México. Nature, 345, 336-338.

Suárez, G., Ligorrea, J.P., Ponce, L., 1992. Preliminary crustal structure of the coast of Guerrero, Mexico, using the minimum apparent velocity of refracted waves. Geofísica Internacional, 31(2), 247-252.

UNAM Seismology Group, 2015. Papanoa, Mexico earthquake of 18 April 2014 (M W 7.3). Geofísica Internacional, 54(4), 363-386.

Wessel, P., Smith, W.H.F., 1991. Free software helps map and display data. EOS Transactions: American Geophysical Union, 72, 41, 441-446.

Zuñiga, F. R., Gutiérrez, C., Nava, E., Lermo, J., Rodriguez, M., Coyoli, R., 1993. Aftershocks of the San Marcos earthquake of April 25, 1989 (Ms=6.9) and some implications for the Acapulco–San Marcos, Mexico, Seismic Potential, Pure and Applied Geophysics, 140, 287-300.

Manuscript received August 2022;
revision accepted September 2023;
published Online November 2023.